Novel high-T_g poly(amine-imide)s bearing pendent *N*-phenylcarbazole units: synthesis and photophysical, electrochemical and electrochromic properties

Guey-Sheng Liou,*[a] Sheng-Huei Hsiao[b] and Hwei-Wen Chen[a]

Received 13th February 2006, Accepted 9th March 2006
First published as an Advance Article on the web 28th March 2006
DOI: 10.1039/b602133f

A new carbazole-derived, triphenylamine-containing aromatic diamine monomer, 4,4′-diamino-4″-*N*-carbazolyltriphenylamine, was successfully synthesized by the caesium fluoride-mediated condensation of *N*-(4-aminophenyl)carbazole with 4-fluoronitrobenzene, followed by palladium-catalyzed hydrazine reduction. A series of novel poly(amine-imide)s **6a–6g** with pendent *N*-phenylcarbazole units having inherent viscosities of 0.17–0.56 dL g^{-1} were prepared from the newly synthesized diamine monomer and seven commercially available tetracarboxylic dianhydrides *via* a conventional two-step procedure that included a ring-opening polyaddition to give polyamic acids, followed by chemical or thermal cyclodehydration. The polymers of the series were amorphous and most of them could afford flexible, transparent, and tough films with good mechanical properties. All the poly(amine-imide)s had useful levels of thermal stability associated with high glass-transition temperatures (303–371 °C), 10% weight-loss temperatures in excess of 543 °C, and char yields at 800 °C in nitrogen higher than 60%. The poly(amine-imide)s **6e–6g** exhibited a UV-vis absorption maximum at around 300 nm in NMP solution. The poly(amine-imide) **6g** derived from an aliphatic dianhydride was optically transparent in the visible region and fluoresced violet–blue at 403 nm in NMP with 4.54% quantum yield higher than the wholly aromatic **6e** and **6f**. The hole-transporting and electrochromic properties were examined by electrochemical and spectroelectrochemical methods. Cyclic voltammograms of the poly(amine-imide) films on an indium-tin oxide (ITO)-coated glass substrate exhibited a reversible oxidation wave at 1.05 V and an additional irreversible oxidation wave at 1.39 V *versus* Ag/AgCl in acetonitrile solution. The polymer films revealed excellent stability of electrochromic characteristics, with a color change from neutral pale yellowish to green doped form at applied potentials ranging from 0.00 to 1.15 V.

Introduction

Triarylamines have attracted considerable interest as hole transport materials for use in multilayer organic electroluminescence (EL) devices due to their relatively high mobilities and their low ionization potentials.[1] The feasibility of utilizing spin-coating and ink-jet printing processes for large-area EL devices and possibilities of various chemical modifications (to improve emission efficiencies and allow patterning) make polymeric materials containing triarylamine units very attractive.[2] To enhance the hole injection ability of polymeric emissive materials such as poly(1,4-phenylenevinylene)s (PPV) and polyfluorenes (PF), there have been several reports on PPV and PF derivatives involving hole-transporting units such as triarylamine or carbazole groups in the emissive π-conjugated core/main chains[3] or grafting them as side chains in a polymer[4] or attaching them onto the polymer chain-ends or the outer surface of dendritic wedges.[5]

Carbazole is a conjugated unit that has interesting optical and electronic properties such as photoconductivity and photorefractivity.[6,7] In the field of electroluminescence, carbazole derivatives are often used as the materials for hole-transporting and light-emitting layers because of their high charge mobility and thermal stability, and show blue electroluminescence due to the large band gap of the improved planar biphenyl unit by the bridging nitrogen atom.[8] From a structural point of view, carbazole differs from diphenylamine in its planar structure since it can be further imagined as bonded diphenylamine; the thermal stability of materials with the incorporation of carbazolyl units therefore was improved. In addition, carbazole can be easily functionalized at the (3,6),[9,10] (2,7)[11] or *N*-positions,[12–14] and then covalently linked into polymeric systems, both in the main-chain[15] as building blocks and in the side-chain as pendent groups.[16] It is thus worthwhile to explore the feasibility of new carbazole-based aromatic diamines as starting monomers for the preparation of high-performance polyimide systems with novel optoelectronic functions.

Aromatic polyimides are well accepted as advanced materials for thin-film applications in microelectronic devices and liquid crystal displays due to their outstanding mechanical,

[a]*Department of Applied Chemistry, National Chi Nan University, 1 University Road, Puli, Nantou Hsien 545, Taiwan, Republic of China. E-mail: gsliou@ncnu.edu.tw*
[b]*Department of Chemical Engineering, Tatung University, 40 Chungshan North Rd. 3rd Sec., Taipei 104, Taiwan, Republic of China*

chemical, thermal, and physical properties.[17] However, the technological applications of most polyimides are limited by processing difficulties because of high melting or glass transition temperatures and limited solubility in most organic solvents due to their rigid backbones. To overcome these limitations, polymer-structure modification becomes necessary. One of the common approaches for increasing solubility and processability of polyimides without sacrificing high thermal stability is the introduction of bulky, packing-disruptive groups into the polymer backbone.[18] Recently, we have reported the synthesis of soluble aromatic polyimides bearing triphenylamine units in the main chain based on *N*,*N*′-bis(4-aminophenyl)-*N*,*N*′-diphenyl-1,4-phenylenediamine[19] and *N*,*N*-bis(4-aminophenyl)-*N*′,*N*′-diphenyl-1,4-phenylenediamine.[20] Because of the incorporation of bulky, propeller-shaped triphenylamine units along the polymer backbone, all the polymers were amorphous, showed good solubility in many aprotic solvents, good film-forming capability, and exhibited high thermal stability.

The electrochemistry of triphenylamine in aprotic solvents has been well studied.[21] The triphenylamine cationic radical of the first electron oxidation is not stable, chemical reaction therefore follows to produce tetraphenylbenzidine by tail-to-tail (*para*-positions) coupling with the loss of two protons per dimer. When the phenyl groups were incorporated by electron-donating substituents at the *para*-position of triarylamines, the coupling reactions were greatly prevented, thus affording stable cationic radicals.[22,23] In this article, we therefore synthesized the novel carbazole-based diamine monomer, 4,4′-diamino-4″-*N*-carbazolyltriphenylamine (**4**), and its derived poly(amine-imide)s containing electron-rich triphenylamine groups with carbazolyl *para*-substituted on the pendent phenyl ring. The general properties such as solubility, crystallinity, and thermal and mechanical properties are described. The electrochemical, electrochromic, and photoluminescent properties of these polymers are also investigated herein and are compared with those of structurally related ones from *N*,*N*-bis(4-aminophenyl)-*N*′,*N*′-diphenyl-1,4-phenylenediamine.[20]

Experimental

Materials

N,*N*-Bis(4-aminophenyl)-*N*′,*N*′-diphenyl-1,4-phenylenediamine (mp = 245–248 °C) was synthesized by the condensation of 4-aminotriphenylamine with 4-fluoronitrobenzene in the presence of sodium hydride, followed by the hydrazine Pd/C-catalyzed reduction of the intermediate dinitro compound according to a previously reported procedure.[20] *N*,*N*-Dimethylacetamide (DMAc) (TEDIA), *N*,*N*-dimethylformamide (DMF) (Acros), dimethyl sulfoxide (DMSO) (TEDIA), and *N*-methyl-2-pyrrolidinone (NMP) (TEDIA) were used without further purification. Commercially available tetracarboxylic dianhydrides such as pyromellitic dianhydride (PMDA) (**5a**) (Chriskev), 3,3′,4,4′-benzophenonetetracarboxylic dianhydride (BTDA) (**5c**) (Chriskev), 4,4′-oxydiphthalic dianhydride (ODPA) (**5d**) (TCI), 3,3′,4,4′-diphenylsulfonetetracarboxylic dianhydride (DSDA) (**5e**) (TCI), and 1,2,3,4-cyclopentanetetracarboxylic dianhydride (CPDA) (**5g**) (TCI) were purified by recrystallization from acetic anhydride. 3,3′,4,4′-Biphenyltetracarboxylic dianhydride (BPDA) (**5b**) (Chriskev) and 2,2-bis(3,4-dicarboxyphenyl)hexafluoropropane dianhydride (6FDA) (**5f**) (Chriskev) were purified by vacuum sublimation. Tetrabutylammonium perchlorate (TBAP) (Acros) was recrystallized twice from ethyl acetate and then dried *in vacuo* prior to use. All other reagents were used as received from commercial sources.

Synthesis of monomer

***N*-(4-Nitrophenyl)carbazole (1).** To a solution of 16.72 g (0.10 mol) of carbazole and 15.52 g (0.11 mol) of 4-fluoronitrobenzene in 70 mL of dried DMSO, 36.46 g (0.24 mol) of dried caesium fluoride was added with stirring all at once, and the mixture was heated at 150 °C for 15 h under nitrogen atmosphere. The mixture was poured into 560 mL of stirred methanol slowly, and the precipitated yellow crystals were collected by filtration and washed thoroughly with methanol. The product was filtered to afford 28.25 g (98% in yield) of yellow crystals with a mp of 209–210 °C (measured by DSC at 10 °C min^{-1}) (lit.[24] 209–211 °C; lit.[25] 120–122 °C). IR (KBr): 1592, 1347 cm^{-1} (–NO_2 stretch). ^{1}H NMR (DMSO-d_6, δ, ppm): 7.33 (t, 3H, H_e), 7.45 (t, 3H, H_d), 7.55 (d, 2H, H_c), 7.96 (d, 2H, H_b), 8.26 (d, 2H, H_f), 8.49 (d, 2H, H_a). ^{13}C NMR (DMSO-d_6, δ, ppm): 109.8 (C^6), 120.5 (C^8), 121.0 (C^9), 123.5 (C^{10}), 125.4 (C^2), 126.4 (C^7), 127.0 (C^3), 139.4 (C^5), 143.0 (C^1), 145.6 (C^4). Anal. Calcd for $C_{18}H_{12}N_2O_2$ (288.30): C, 74.99%; H, 4.20%; N, 9.72%. Found: C, 74.96%; H, 4.27%; N, 9.85%.

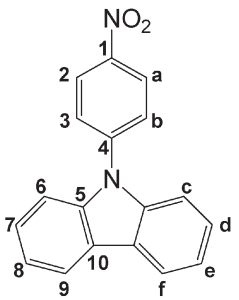

***N*-(4-Aminophenyl)carbazole (2).** In a 500 mL round-bottom flask equipped with a stirring bar, 28.83 g (0.10 mol) of nitro compound **1** and 0.70 g of 10% Pd/C were dissolved/suspended in 300 mL of ethanol. The suspension solution was heated to reflux, and 15 mL of hydrazine monohydrate was added slowly to the mixture, then the solution was stirred at reflux temperature. After a further 9 h of reflux, the solution was filtered hot to remove Pd/C, and the filtrate was evaporated under reduced pressure to dryness. A yellowish syrup was obtained. The product was used for the next step without further purification. IR (KBr): 3368, 3448 cm^{-1} (N–H stretch). ^{1}H NMR (DMSO-d_6, δ, ppm): 6.80 (d, 2H, H_a), 7.17–7.26 (m, 5H, H_b + H_c + H_e), 7.36 (d, 2H, H_d), 8.17 (d, 2H, H_f), 5.44 (s, 2H, NH_2). ^{13}C NMR (DMSO-d_6, δ, ppm): 109.8 (C^6), 114.9 (C^2), 119.5 (C^8), 120.5 (C^9), 122.4 (C^{10}), 124.7 (C^4), 126.1 (C^7), 127.9 (C^3), 141.1 (C^5), 148.8 (C^1). Anal. Calcd for $C_{18}H_{14}N_2$

(258.32): C, 83.69%; H, 5.46%; N, 10.84%. Found: C, 83.29%; H, 5.50%; N, 10.74%.

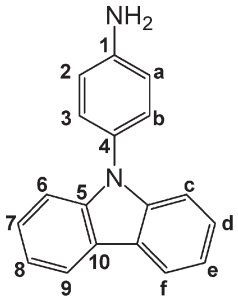

4,4′-Dinitro-4″-*N*-carbazolyltriphenylamine (3). To a solution of 18.08 g (0.07 mol) of compound **2** and 21.73 g (0.15 mol) of 4-fluoronitrobenzene in 100 mL of dried DMSO, 25.52 g (0.17 mol) of dried caesium fluoride was added with stirring all at once, and the mixture was heated at 150 °C for 15 h under nitrogen atmosphere. The mixture was poured into 1 L of saturated aqueous NaCl solution to give orange–red solids. The crude product was further purified by recrystallization from DMF affording orange–red needles with a mp of 302–305 °C (by DSC) in 78% yield (27.33 g). IR (KBr): 1579, 1307 cm^{-1} (NO_2 stretch). Anal. Calcd for $C_{30}H_{20}N_4O_4$ (500.50): C, 71.99%; H, 4.03%; N, 11.19%. Found: C, 71.94%; H, 3.96%; N, 11.28%. Crystal data for **3**: orange-red single crystal grew by the slow crystallization from DMF, crystal dimensions: 0.50 × 0.44 × 0.33 mm^3, triclinic, space group $P\bar{1}$, a = 9.254(6) Å, b = 11.130(8) Å, c = 12.368(8) Å, α = 100.153(12)°, β = 97.120(13)°, γ = 98.744(13)°, D_{calcd} = 1.358 Mg m^{-3}, Z = 2, and V = 1224.4(14) $Å^3$.

4,4′-Diamino-4″-*N*-carbazolyltriphenylamine (4). In a 500 mL round-bottom flask equipped with a stirring bar, 7.04 g (14.00 mmol) of dinitro compound **3** and 1.00 g of 10% Pd/C were dissolved/suspended in 400 mL of ethanol. The suspension solution was heated to reflux, and 18 mL of hydrazine monohydrate was added slowly to the mixture, then the solution was stirred at reflux temperature. After a further 9 h of reflux, the solution was filtered hot to remove Pd/C, and the filtrate was then cooled to precipitate white needles. The product was collected by filtration and washed with ethanol, and dried *in vacuo* at 80 °C to give 4.80 g (79% in yield) of white needles with a mp of 192–195 °C (by DSC). IR (KBr): 3357, 3436 cm^{-1} (N–H stretch). ^{1}H NMR (DMSO-d_6, δ, ppm): 6.65 (d, 4H, H_h), 6.82 (d, 2H, H_a), 6.99 (d, 4H, H_g), 7.23 (t, 4H, H_b + H_e), 7.30 (d, 2H, H_c), 7.39 (t, 2H, H_d), 8.18 (d, 2H, H_f), 5.04 (s, 4H, NH_2). ^{13}C NMR (DMSO-d_6, δ, ppm): 109.6 (C^6), 115.0 (C^{13}), 116.5 (C^2), 119.5 (C^8), 120.3 (C^9), 122.3 (C^{10}), 125.9 (C^7), 126.0 (C^1), 127.2 (C^3), 127.8 (C^{12}), 135.4 (C^{11}), 140.7 (C^5), 146.0 (C^{14}), 149.1 (C^4). Anal. Calcd for $C_{30}H_{24}N_4$ (440.55): C, 81.79%; H, 5.49%; N, 12.72%. Found: C, 81.72%; H, 5.41%; N, 12.63%. Crystal data for **4**·THF: colorless single crystal (a crystallosolvate with THF) grew by slow evaporation of its tetrahydrofuran (THF)–ethanol solution, crystal dimensions: 0.70 × 0.60 × 0.50 mm^3, triclinic, space group $P\bar{1}$, a = 11.242(2) Å, b = 11.818(2) Å, c = 11.950(2) Å, α = 100.705(10)°, β = 105.972(10)°, γ = 113.247(10)°, where the density of crystal D_{calcd} = 1.288 Mg m^{-3} for Z = 2 and V = 1322.28(4) $Å^3$.

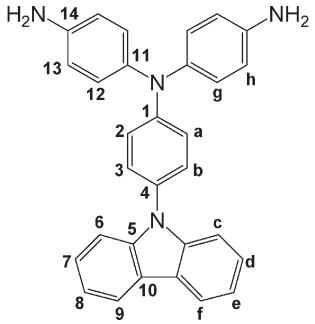

4,4′-Diphthalimido-4″-*N*-carbazolyltriphenylamine (4a). To a solution of 0.18 g (0.40 mmol) of compound **4** was added 0.13 g (0.85 mmol) of phthalic anhydride in 2 mL of dried DMF with stirring all at once. The mixture was stirred for 4 h, followed by the addition of acetic anhydride 0.75 mL and pyridine 0.3 mL. After being stirred for 2 h at room temperature, the mixture was heated at 90 °C for 4 h. The yellowish transparent solution was poured into 100 mL of stirred methanol slowly, and the precipitated yellowish powder was collected by filtration to afford 0.27 g (86% yield) of yellowish powders with a mp of 328–331 °C measured by DSC at 10 °C min^{-1}. IR (KBr): 1716 (symmetrical C=O), 1383 (C–N), and 714 cm^{-1} (imide ring deformation).

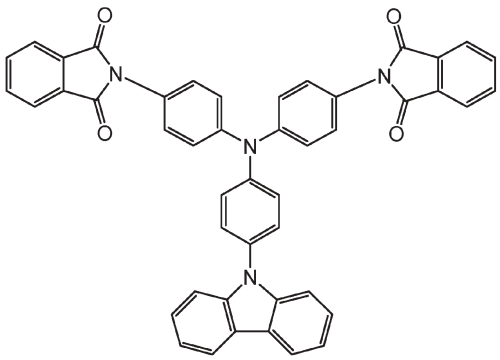

Polymer synthesis. poly(amine-imide)s 6a–6d by two-step method *via* thermal imidization reaction

The poly(amine-imide)s **6a**–**6d** were synthesized from diamine **4** and dianhydrides **5a**–**5d** by the conventional two-step method *via* thermal imidization. The synthesis of poly(amine-imide) **6b** was used as an example to illustrate the general synthetic route used to produce the poly(amine-imide)s. To a solution of 0.60 g (1.36 mmol) of diamine **4** in 9.5 mL of DMAc, 0.40 g (1.36 mmol) of dianhydride BPDA (**5b**) was added in one portion. The mixture was stirred at room temperature overnight (*ca.* 12 h) to afford a viscous poly(amic acid) solution. The inherent viscosity of the resulting poly(amic acid) was 0.98 dL g^{-1}, measured in DMAc at a concentration of 0.5 g dL^{-1} at 30 °C. The poly(amic acid) film was obtained by casting from the reaction polymer solution onto a glass plate and drying at 90 °C under vacuum. The poly(amic acid)

in film form was converted to poly(amine-imide) **6b** by successive heating under vacuum at 100 °C for 1 h, 200 °C for 1 h, and then 300 °C for 1 h. The inherent viscosity of poly(amine-imide) **6b** was 0.56 dL g^{-1}, measured at a concentration of 0.5 g dL^{-1} in concentrated sulfuric acid at 30 °C. Anal. Calcd for $(C_{46}H_{26}N_4O_4)_n$ (698.72)$_n$: C, 79.07%; H, 3.75%; N, 8.02%. Found: C, 77.70%; H, 3.77%; N, 7.85%.

Poly(amine-imide)s 6e–6g by two-step method *via* chemical imidization reaction

The poly(amine-imide)s **6e**–**6g** were synthesized from diamine **4** and dianhydrides **5e**–**5g** by the conventional two-step method *via* chemical imidization. The synthesis of poly(amine-imide) **6e** was used as an example to illustrate the general synthetic route used to produce the poly(amine-imide)s. To a solution of 0.55 g (1.25 mmol) of diamine **4** in 9.5 mL of DMAc, 0.45 g (1.25 mmol) of dianhydride DSDA (**5e**) was added in one portion. The mixture was stirred at room temperature overnight (*ca.* 12 h) to afford a viscous poly(amic acid) solution. The inherent viscosity of the resulting poly(amic acid) was 0.98 dL g^{-1}, measured in DMAc at a concentration of 0.5 g dL^{-1} at 30 °C. The poly(amic acid) was subsequently converted to poly(amine-imide) **6e** *via* a chemical imidization process by addition of pyridine 2 mL and acetic anhydride 5 mL, and the mixture was heated at 100 °C for 2 h to effect complete imidization. The resulting polymer solution was poured into 300 mL of methanol giving a fibrous precipitate, which was washed thoroughly with methanol, and collected by filtration. The precipitate was dissolved in 8 mL of NMP, and the homogeneous solution was poured into a 9 cm glass culture dish, which was placed in a 90 °C oven for 12 h to remove the solvent. Then, the obtained film was further dried *in vacuo* at 150 °C for 6 h. The inherent viscosity of poly(amine-imide) **6e** was 0.47 dL g^{-1} in NMP at a concentration of 0.5 g dL^{-1} at 30 °C. Anal. Calcd for $(C_{46}H_{26}N_4O_6S)_n$ (762.79)$_n$: C, 72.43%; H, 3.44%; N, 7.35%; S, 4.20%. Found: C, 71.62%; H, 3.66%; N, 7.34%; S, 4.25%.

Measurements

Infrared spectra were recorded on a Perkin Elmer RXI FT-IR spectrometer. Elemental analyses were run in a VarioEL-III Elementar. ^{1}H and ^{13}C NMR spectra were measured on a Bruker AV-500 FT-NMR system. X-Ray single-crystal diffraction experiments were carried on a Norius Kappa CCD four-circle diffractometer equipped with graphite-monochromated Mo-Kα radiation. The structures were solved by direct methods using SHELXL-97 software (Sheldrick, 1997). The inherent viscosities were determined at 0.5 g dL^{-1} concentration using a Tamson TV-2000 viscometer at 30 °C. Wide-angle X-ray diffraction (WAXD) measurements were performed at room temperature (*ca.* 25 °C) on a Shimadzu XRD-7000 X-ray diffractometer (40 kV, 20 mA), using graphite-monochromatized Cu-Kα radiation. Ultraviolet-visible (UV-vis) spectra of the polymer films were recorded on a Varian Cary 50 Probe spectrometer. An Instron universal tester model 4400R with a 5 kg load cell was used to study the stress–strain behavior of the samples. A gauge length of 2 cm and a crosshead speed of 5 mm min^{-1} were used for this study. Measurements were performed at room temperature with film specimens (0.5 cm width, 6 cm length), and an average of at least three replicates was used. Thermogravimetric analysis (TGA) was conducted with a Perkin Elmer Pyris 1 TGA. Experiments were carried out on approximately 6–8 mg film samples heated in flowing nitrogen or air (flow rate = 20 cm^3 min^{-1}) at a heating rate of 20 °C min^{-1}. DSC analyses were performed on a Perkin Elmer Pyris Diamond DSC at a scan rate of 20 °C min^{-1} in flowing nitrogen (20 cm^3 min^{-1}). Thermomechanical analysis (TMA) was conducted with a Perkin Elmer TMA 7 instrument. The TMA experiments were conducted from 50 to 350 °C at a scan rate of 10 °C min^{-1} with a penetration probe 1.0 mm in diameter under an applied constant load of 10 mN. Softening temperatures (T_s) were taken as the onset temperatures of probe displacement on the TMA traces. Cyclic voltammetry was performed with a Bioanalytical System Model CV-27 potentiostat and a BAS X-Y recorder with ITO (polymer films area about 0.7 cm × 0.5 cm) as a working electrode and a platinum wire as an auxiliary electrode at a scan rate of 100 mV s^{-1} against a Ag/AgCl reference electrode in a solution of 0.1 M tetrabutylammonium perchlorate (TBAP)–acetonitrile (CH_3CN). Voltammograms are presented with the positive potential pointing to the left and with increasing anodic currents pointing downwards. The spectroelectrochemical cell was composed of a 1 cm cuvette, ITO as a working electrode, a platinum wire as an auxiliary electrode, and a Ag/AgCl reference electrode. Absorption spectra in spectroelectrochemical analysis were measured with a HP 8453 UV-Visible spectrophotometer. Photoluminescence spectra were measured with a Jasco FP-6300 spectrofluorometer. Fluorescence quantum yields (Φ_F) of the samples in NMP were measured by using quinine sulfate in 1 N H_2SO_4 as a reference standard (Φ_F = 0.546).[26] All corrected fluorescence excitation spectra were found to be equivalent to their respective absorption spectra.

Results and discussion

Monomer synthesis

N-(4-Aminophenyl)carbazole (**2**)[24] was prepared by the caesium fluoride-mediated aromatic nucleophilic substitution reaction of carbazole with 4-fluoronitrobenzene followed by hydrazine Pd/C-catalytic reduction according to the synthetic route outlined in Scheme 1. The new aromatic diamine having a bulky pendent *N*-phenylcarbazole group, 4,4′-diamino-4″-*N*-carbazolyltriphenylamine (**4**), was successfully synthesized by hydrazine Pd/C-catalyzed reduction of the dinitro compound **3** resulting from double *N*-arylation reaction of compound **2** with 4-fluoronitrobenzene in the presence of caesium fluoride. Elemental analysis, IR, and ^{1}H and ^{13}C NMR spectroscopic techniques were used to identify structures of the intermediate compounds **1**, **2**, and **3** and the target diamine monomer **4**. Fig. 1 illustrates the ^{1}H NMR and ^{13}C NMR spectra of the diamine monomer **4**. Assignments of each carbon and proton are assisted by the two-dimensional NMR spectra shown in Figs. 2 and 3, and these spectra agree well with the proposed molecular structure of compound **4**. The molecular structures of compounds **3** and **4** were further

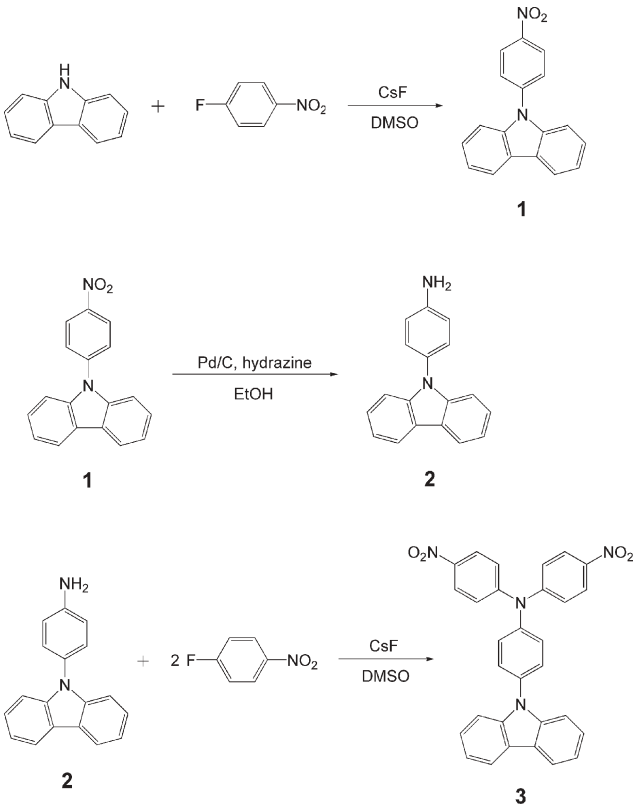

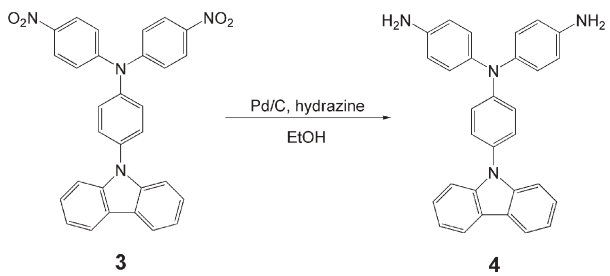

Scheme 1

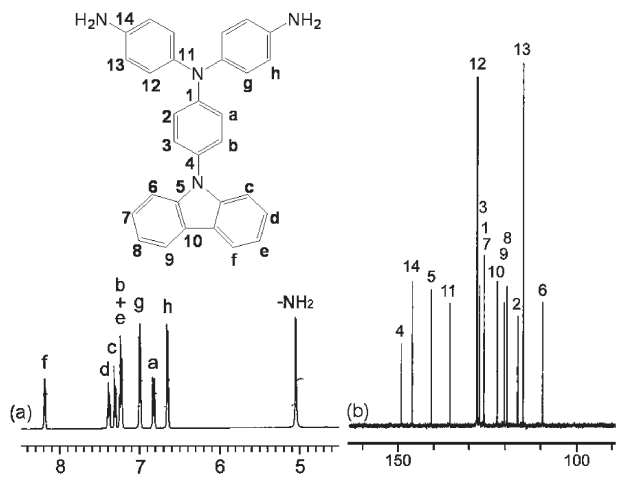

Fig. 1 (a) ^{1}H NMR and (b) ^{13}C NMR spectra of compound **4** in DMSO-d_6.

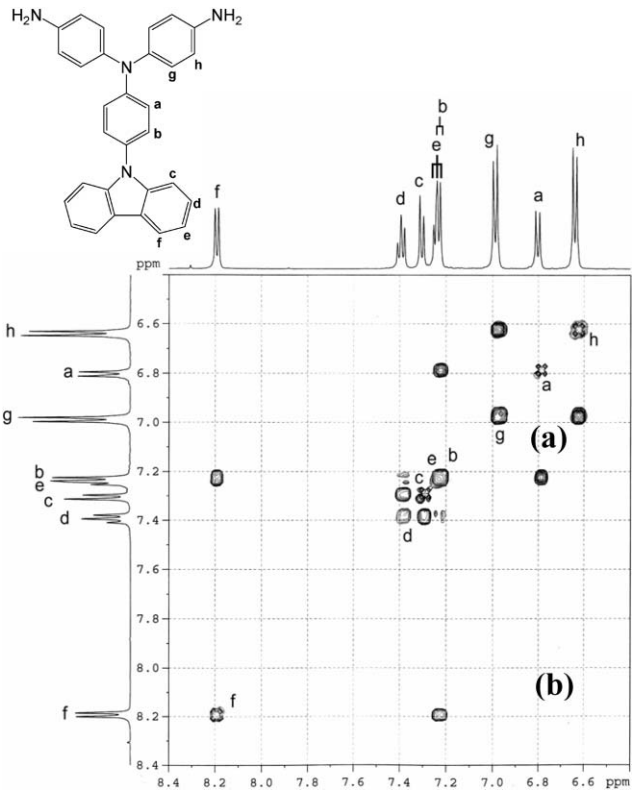

Fig. 2 H–H COSY spectrum of diamine **4** in DMSO-d_6.

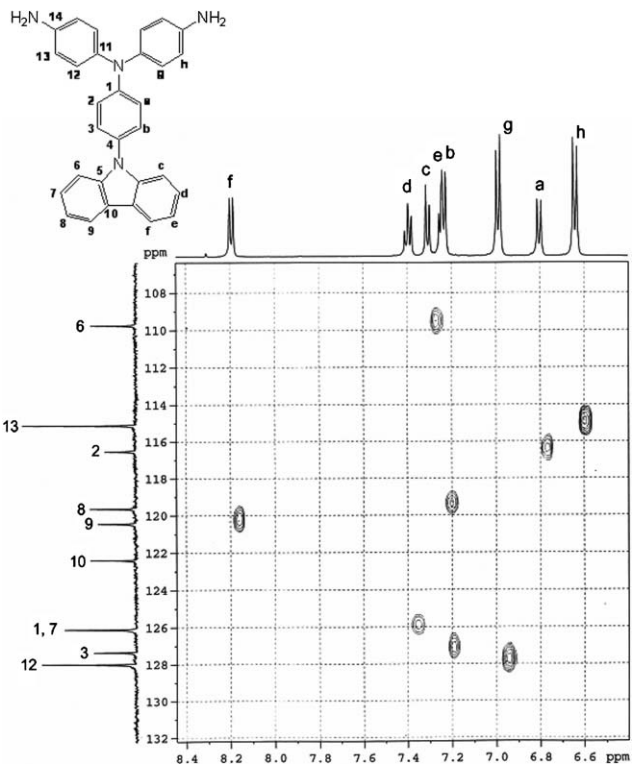

Fig. 3 C–H COSY spectrum of diamine **4** in DMSO-d_6.

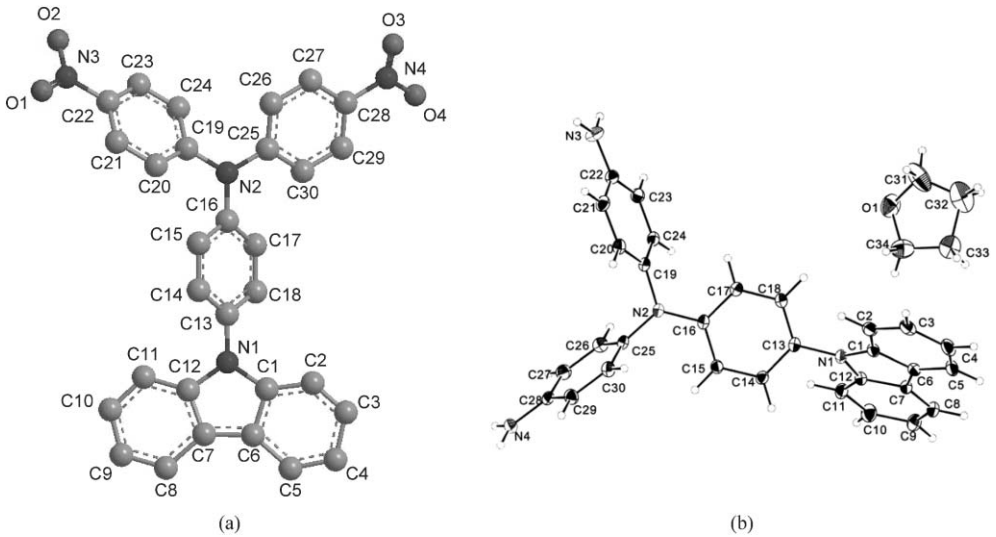

Fig. 4 X-Ray structures of (a) dinitro compound **3** and (b) the crystalline solvate of diamine monomer **4** with THF.

confirmed by single-crystal X-ray diffractions (Fig. 4). The single crystals of **3** were acquired by slow crystallization of a DMF solution. On the other hand, the crystal of **4** contains THF, one of the components of the mixed solvents, in a ratio of 1 : 1 with **4**, as shown in Fig. 4(b). The molecular structure of **4** is very similar to that of **3** apart from replacement of nitro by amino substituents. As shown in Fig. 4, the molecular structures display a coplanar structure of the carbazolyl unit and a propeller-shaped conformation of the triphenylamine core.

Polymer synthesis

A series of novel poly(amine-imide)s **6a**–**6g** bearing pendent *N*-phenylcarbazole units were prepared by the reaction of diamine **4** with seven commercially available dianhydrides **5a**–**5g** in DMAc at room temperature to form the precursor poly(amic acid)s, followed by chemical or thermal imidization (Scheme 2). In the first step, the viscosities of the reaction mixtures became very high as poly(amic acid)s were formed, indicating the formation of high molecular weight polymers. The thermal conversion to polyimides was carried out by successive heating of the poly(amic acid) films to 300 °C *in vacuo*. The poly(amic acid) precursors also could be chemically dehydrated to the polyimides by treatment with acetic anhydride and pyridine. All poly(amine-imide)s could afford good, free-standing films, although the films of **6a** and **6g** might crack on fingernail creasing because of structural rigidity or lower molecular weight (for **6g**). The formation of poly(amine-imide)s was confirmed with elemental analysis, IR, and NMR spectroscopy. The inherent viscosities and elemental analysis data of these poly(amine-imide)s are summarized in Table 1. The IR spectra of these polymers exhibited characteristic imide absorption bands at around 1775 (symmetrical C=O), 1716 (symmetrical C=O), 1383 (C–N), and 714 cm^{-1} (imide ring deformation). The microstructures of these poly(amine-imide)s were also verified by the high-resolution NMR spectra. For a comparative study, a series of referenced poly(amine-imide)s **6′a**–**6′g** were also synthesized from *N*,*N*-bis(4-aminophenyl)-*N′*,*N′*-diphenyl-1,4-phenylenediamine and dianhydrides **5a**–**5g**.

Basic characterization

The color of polyimide films depends markedly on the chemical structure of the dianhydride components (Table 1). The colors of poly(amine-imide) **6a**–**6f** films were from yellowish to deep reddish or brownish that could be attributed to charge-transfer complex (CTC) formation between the electron-donating amino unit and the strongly electron-accepting pyromellitimide or phthalimide unit. Due to effective diminution of the conjugation and intermolecular CTC formation by aliphatic tetracarboxylic dianhydride (CPDA), the film of poly(amine-imide) **6g** was less colored.[27] As mentioned previously, the poly(amine-imide)s **6b**–**6f** could afford flexible, transparent, and tough films. These films were subjected to tensile testing, and the results are given in Table 2. The tensile strengths, elongations to break, and initial moduli of these films were in the ranges of 71–110 MPa, 6–18% and 2.1–3.0 GPa, respectively. The WAXD studies of the poly(amine-imide)s indicated that all the polymers were essentially amorphous. The amorphous nature can be attributed to the introduction of bulky, twisted, three-dimensional *N*-carbazolyl-substituted triphenylamino units along the polymer backbone.

The solubility behavior of polymers **6a**–**6g** obtained by thermal or chemical imidization was investigated qualitatively, and the results are listed in Table 3. The solubility behavior of the polyimides depended on their chain packing ability and intermolecular interactions that was affected by the rigidity, symmetry, and regularity of the molecular backbone. Except for poly(amine-imide)s derived from more rigid dianhydrides, such as **5a**–**5d**, the other poly(amine-imide)s **6e**–**6f** exhibited higher solubility in polar aprotic organic solvents such as NMP, DMAc, DMF, and *m*-cresol. The poly(amine-imide)s **6f** and **6g** were soluble not only in polar aprotic organic solvents but also in less polar solvents such as chloroform and THF. Their excellent solubility can be attributable to the existence of

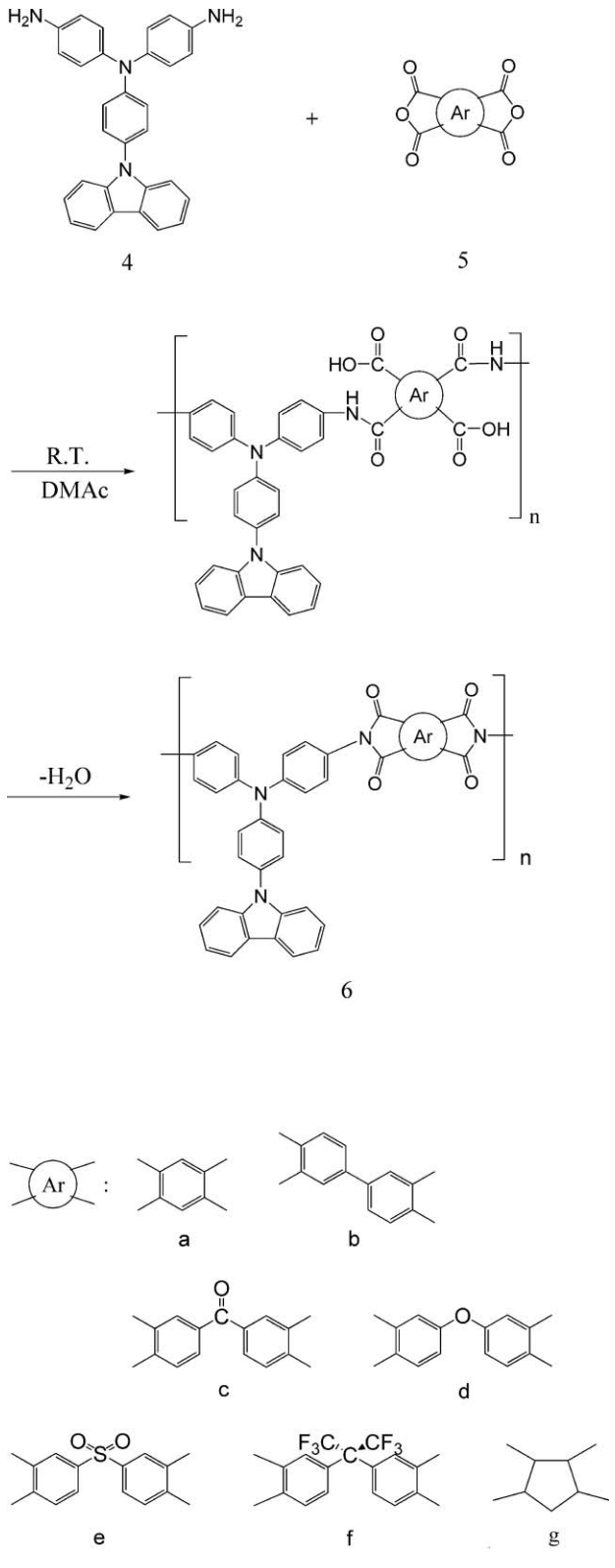

Scheme 2

the hexafluoroisopropylidene and alicyclic structure which limit the CTC formation and reduce the intermolecular interactions. In addition, the poly(amine-imide)s prepared by the chemical imidization method had better solubility as compared with those by the two-step thermal imidization method. Thus, the difference in solubility of poly(amine-imide)s obtained by different methods could be ascribed to morphological change of the polymers during heat treatment resulting in some degree of ordering from molecular aggregation of the polymer chain segments.

The thermal properties of these poly(amine-imide)s are summarized in Table 4. Typical TGA curves for poly(amine-imide) **6c** and **6′c** are reproduced in Fig. 5. All of the poly(amine-imide)s exhibited a similar TGA pattern with no significant weight loss below 500 °C in air or nitrogen atmosphere. The 10% weight-loss temperatures of the poly(amine-imide)s in nitrogen and air were recorded in the range of 543–652 °C and 549–634 °C, respectively. The amount of carbonized residue (char yield) of these polymers in nitrogen atmosphere was more than 60% at 800 °C. The high char yields of these polymers can be ascribed to their high aromatic content. The relatively lower stability of **6g** is reasonable when considering its less stable aliphatic segments. The glass-transition temperatures (T_gs) of all the polymers were observed in the range of 303–371 °C by DSC and decreased with decreasing rigidity and symmetry of the aromatic tetracarboxylic dianhydride. As shown in Table 4, the thermal properties compared with the analogous poly(amine-imide)s **6′a**–**6′f**, the **6** series of poly(amine-imide)s showed an increased T_g and an enhanced thermal stability (Fig. 5) because of the decreased conformational flexibility or free volume caused by the introduction of planar carbazole groups in the repeat unit. All the polymers indicated no clear melting endotherms up to the decomposition temperatures on the DSC thermograms. The softening temperatures (T_s) (may be referred to as apparent T_g) of the polymer film samples were determined by the TMA method with a loaded penetration probe. They were obtained from the onset temperature of the probe displacement on the TMA trace. A typical TMA thermogram for poly(amine-imide) **6e** is illustrated in Fig. 6. In most cases, the T_s values obtained by TMA are comparable to the T_g values measured by the DSC experiments (Table 4).

Optical and electrochemical properties

The optical and electrochemical properties of the poly(amine-imide)s were investigated by UV-vis and photoluminescence (PL) spectroscopy and cyclic voltammetry. The results are summarized in Table 5. The organosoluble polymers **6e**–**6g** exhibited UV-vis absorption bands with λ_{max} at 295–340 nm in NMP solutions, assignable to the π–π* transition resulting from the conjugation between the aromatic rings and nitrogen atoms that combines the characteristic π–π* transitions of triphenylamine moieties (295–310 nm) and carbazole chromophores (320–340 nm).[25] In the solid film, the poly(amine-imide)s showed absorption characteristics (λ_{max} around 320–330 nm) similar to those in the solution. Fig. 7 shows solution UV-vis absorption and PL emission spectra of poly(amine-imide)s **6e–g** in NMP at a concentration of around 1×10^{-5} mol L^{-1}. These carbazole-based poly(amine-imide)s exhibited a violet–blue fluorescence emission maximum at around 402–455 nm in the NMP solution. The fluorescence quantum yield in NMP solution ranges from 0.61% for **6f** to 4.54% for **6g**. The blue shift and higher fluorescence quantum

Table 1 Inherent viscosity and elemental analysis of poly(amine-imide)s

Poly(amine-imide)s			Elemental analysis (%) of poly(amine-imide)s					
Code	η_{inh}[a]/dL g^{-1}	Color of film[b]	Formula (formula weight)		C	H	N	S
6a	0.45	dark brown	$(C_{40}H_{22}N_4O_4)_n$ (622.63)$_n$	Calcd	77.16	3.56	9.00	
				Found	75.49	3.75	8.97	
6b	0.56	dark orange	$(C_{46}H_{26}N_4O_4)_n$ (698.72)$_n$	Calcd	79.07	3.75	8.02	
				Found	77.70	3.77	7.85	
6c	0.33	orange–red	$(C_{47}H_{26}N_4O_5)_n$ (726.73)$_n$	Calcd	77.68	3.61	7.71	
				Found	77.46	3.91	7.95	
6d	0.46	yellow–brown	$(C_{46}H_{26}N_4O_5)_n$ (714.72)$_n$	Calcd	77.30	3.67	7.84	
				Found	76.27	3.81	7.79	
6e	0.47	orange–red	$(C_{46}H_{26}N_4O_6S)_n$ (762.79)$_n$	Calcd	72.43	3.44	7.35	4.20
				Found	71.62	3.66	7.34	4.25
6f	0.55	yellow–brown	$(C_{49}H_{26}F_6N_4O_4)_n$ (848.75)$_n$	Calcd	69.34	3.09	6.60	
				Found	67.40	3.28	6.22	
6g	0.17	off-white	$(C_{39}H_{26}N_4O_4)_n$ (614.65)$_n$	Calcd	76.21	4.26	9.12	
				Found	74.10	4.78	9.00	

[a] Measured at a polymer concentration of 0.5 g dL^{-1} in NMP at 30 °C (**6a**, **6b**, **6c**, and **6d** measured in concentrated sulfuric acid). [b] Thickness: **6a**–**6f**: 60–90 μm; **6g**: 4 μm.

Table 2 Mechanical properties of poly(amine-imide) films

Polymer	Tensile strength/MPa	Elongation at break (%)	Initial modulus/GPa
6b	129	18	2.0
6c	101	8	2.1
6d	83	6	2.3
6e	110	6	3.0
6f	87	9	1.9

yield of light-colored **6g** compared to **6e**–**6f** could be attributed to the incorporation of aliphatic tetracarboxylic dianhydride (CPDA) into the polymer backbone, which effectively reduce the conjugation and the formation of intermolecular CTC. The photoluminescence of the polymer thin films of **6g** and **6′g** under UV irradiation is shown in Fig. 8, and these two films fluoresce violet and deep blue, respectively. The cutoff wavelengths (absorption edge; λ_0) from the UV-vis transmittance spectra are also included in Table 5. It revealed that most of the visible region can be absorbed by poly(amine-imide)s **6a**, **6c** and **6e** which show higher λ_0 values. This is consistent with the fact that the films of these polymers appeared red–brown to deep brown color as shown in Table 1. In contrast, the poly(amine-imide) **6g** and **6′g** showed a light color and high optical transparency with cutoff wavelength in the range of 340–351 nm due to lower capability of intermolecular CTC formation.

The electrochemical behavior of the **6** and **6′** series of poly(amine-imide)s was investigated by a cyclic voltammetry technique conducted for a cast film on an ITO-coated glass substrate as working electrode in dry acetonitrile (CH_3CN) containing 0.1 M of TBAP as the supporting electrolyte and saturated Ag/AgCl as the reference electrode under nitrogen atmosphere. Fig. 9 shows the typical cyclic voltammograms of poly(amine-imide)s **6f** and **6′f**. All the **6** series poly(amine-imide)s reveal one reversible redox couple at a half-wave potential ($E_{1/2}$) of 1.05–1.10 V and one irreversible oxidation redox wave at $E_{1/2}$ = 1.39–1.44 V under an anodic sweep. The first electron removal for poly(amine-imide) **6f** is assumed to occur at the nitrogen atom on the main chain triphenylamine unit, which is more electron-rich than the nitrogen atom on the pendent carbazolyl moiety. This electrochemical behavior was also evidenced by comparing *N*-phenylcarbazole with the

Table 3 Solubility of poly(amine-imide)s[a]

		Solvent						
Polymer	Method of preparation[b]	NMP	DMAc	DMF	DMSO	*m*-Cresol	THF	Chloroform
6a	two-step (T)	—	—	—	—	—	—	—
	two-step (C)	±	±	±	±	—	—	—
6b	two-step (T)	—	—	—	—	+	—	—
	two-step (C)	±	—	—	—	+	—	—
6c	two-step (T)	S	—	—	S	S	—	—
	two-step (C)	±	—	—	—	+	—	—
6d	two-step (T)	±	—	—	—	—	—	—
	two-step (C)	±	—	—	—	+	—	—
6e	two-step (T)	+	+	+	+	+	—	—
	two-step (C)	++	++	±	+	+	—	—
6f	two-step (T)	++	++	++	+	+	++	++
	two-step (C)	++	++	++	++	+	++	++
6g	two-step (T)	++	++	++	+	+	—	—
	two-step (C)	++	++	++	++	++	++	++

[a] Qualitative solubility was tested with 1 mg of a sample in 1 mL of stirred solvent. ++: soluble at room temperature; +: soluble on heating; ±: partially soluble; S: swelling; —: insoluble even on heating. [b] (T): thermal imidization; (C): chemical imidization.

Table 4 Thermal properties of poly(amine-imide)s[a]

Polymer	T_g/°C[b]	T_s/°C[c]	T_d at 5% weight loss/°C[d]		T_d at 10% weight loss/°C[d]		Char yield (wt%)[e]
			in N_2	in air	in N_2	in air	
6a	371 (352)[f]	353	620	603	640 (624)	627 (610)	72 (68)
6b	325 (302)	324	631	607	652 (629)	634 (622)	74 (70)
6c	312 (294)	304	599	592	623 (618)	621 (589)	68 (63)
6d	303 (264)	299	630	607	648 (610)	627 (600)	73 (74)
6e	326 (305)	328	537	529	614 (568)	584 (582)	68 (67)
6f	310 (286)	304	604	553	642 (585)	576 (574)	72 (68)
6g	345	320	519	483	543	549	60

[a] The polymer film samples were heated at 300 °C for 1 h prior to all the thermal analyses. [b] Midpoint temperature of baseline shift on the second DSC heating trace (rate 20 °C min^{-1}) of the sample after quenching from 400 °C. [c] Softening temperature measured by TMA with a constant applied load of 10 mN at a heating rate of 10 °C min^{-1}. [d] Decomposition temperature, recorded *via* TGA at a heating rate of 20 °C min^{-1} and a gas-flow rate of 30 cm^3 min^{-1}. [e] Residual weight percentage at 800 °C in nitrogen. [f] Data in parentheses are those of structurally similar poly(amine-imide)s **6′a**–**6′f** having the corresponding dianhydride residue as in the **6** series.

6 series: **6'** series[20]:

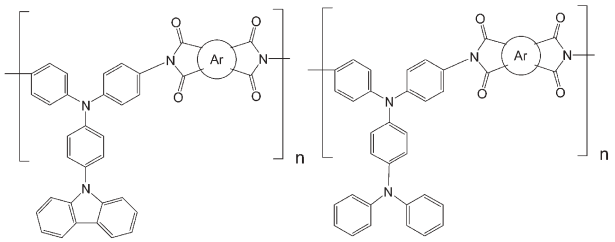

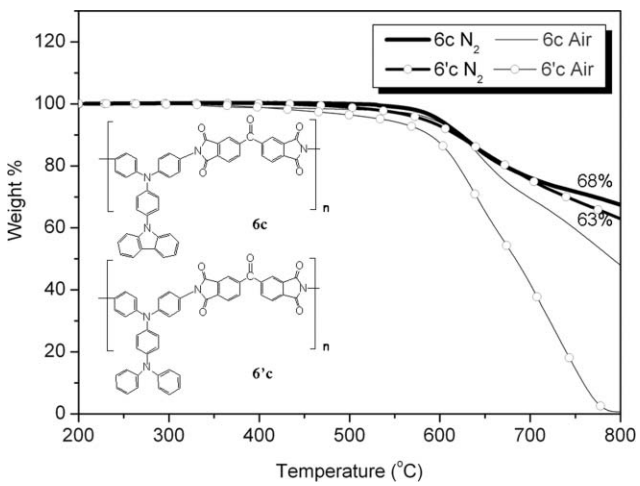

Fig. 5 TGA thermograms of poly(amine-imide) **6c** and **6′c** at a scan rate of 20 °C min^{-1}.

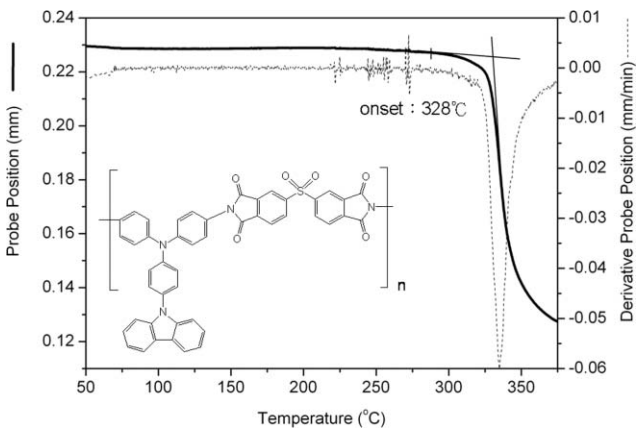

Fig. 6 TMA curve of poly(amine-imide) **6e** with a heating rate of 10 °C min^{-1}.

model compound, 4,4′-diphthalimido-4″-*N*-carbazolyltriphenylamine **4a**. *N*-Phenylcarbazole showed one irreversible peak in CH_3CN ($E_{p,a}$ = 1.35 V). In contrast, the model compound **4a** exhibited a reversible first oxidation at $E_{1/2}$ = 1.09 V and an irreversible second oxidation at $E_{p,a}$ = 1.35 V. The oxidation potential of *N*-phenylcarbazole is similar to the second oxidation potential of model compound **4a** at $E_{p,a}$ = 1.35 V. Thus, the first stable cationic radical of poly(amine-imide)$s^{+\bullet}$ should be formed by the first oxidation at the nitrogen atom of the triphenylamine unit. The energy levels of the HOMO and LUMO of the investigated poly(amine-imide)s can be estimated from the oxidation onset (E_{onset}) or half-wave potentials ($E_{1/2}$) and the onset absorption wavelength of the UV-vis spectra, and the results are listed in Table 5. For example, the oxidation half-wave potential for poly(amine-imide) **6f** has been determined as 1.10 V *vs.* Ag/Ag^+. The external ferrocene/ferrocenium (Fc/Fc^+) redox standard $E_{1/2}$ is 0.44 V *vs.* Ag/Ag^+ in CH_3CN. Assuming that the HOMO energy for the Fc/Fc^+ standard is 4.80 eV with respect to the zero vacuum level, the HOMO energy for poly(amine-imide) **6f** has been evaluated to be 5.46 eV. In comparison, the **6′** series polymers exhibited lower first oxidation potentials and HOMO values than the corresponding **6** series. This could be attributed to the fact that the pendent triphenylamine unit of the **6′** series ($E_{p,a}$ = 0.80 V in CH_3CN)[20] is easier to oxidize than *N*-phenylcarbazole ($E_{p,a}$ = 1.35 V in CH_3CN).

Table 5 Optical and electrochemical properties for poly(amine-imide)s

	Solution λ/nm[b]			Film λ/nm				$E_{1/2}$/V (*vs.* Ag/AgCl in CH_3CN)		E_g[h]/	HOMO[i]/	LUMO[i]/
Index[a]	Abs max.	PL max.	Φ_F (%)[d]	λ_0[e]	Abs max.	Abs onset	PL max.[f]	1st	2nd	eV	eV	eV
6a	—	—	—	628	320	419	—	1.05	(1.44)[g]	2.96	5.41	2.45
6b	—	—	—	530	331	387	—	1.07	(1.42)[g]	3.20	5.43	2.23
6c	—	—	—	543	318	392	—	1.05	(1.40)[g]	3.16	5.41	2.25
6d	—	—	—	488	328	378	—	1.06	(1.42)[g]	3.28	5.42	2.14
6e	295 (340)[c]	455	0.76	534	328	392	—	1.08	(1.43)[g]	3.16	5.44	2.28
6f	295 (341)[c]	431	0.61	485	329	377	—	1.10	(1.44)[g]	3.29	5.46	2.17
6g	295 (340)[c]	402	4.54	351	331	367	398	1.08	(1.39)[g]	3.38	5.44	2.06
6′d	(311)[c]	459	1.10	502	334	397	—	0.79	1.14	3.12	5.15	2.03
6′e	(309)[c]	426	0.30	610	309	405	—	0.81	1.15	3.06	5.17	2.11
6′f	(308)[c]	458	1.04	506	330	393	—	0.81	1.16	3.16	5.17	2.01
6′g	(314)[c]	436	1.57	340	323	388	424	0.73	1.11	3.20	5.09	1.89

[a] **6** and **6′** series as shown in Table 4 footnotes. **6a**–**6a** are difficult to dissolve in NMP. [b] Polymer concentration of 1×10^{-5} mol L^{-1} in NMP. [c] Excitation wavelength. [d] The quantum yield in dilute solution was calculated with quinine sulfate as the standard (Φ_F = 0.546). [e] The cutoff wavelength from the UV-vis transmission spectra of polymer films. [f] They were excited at the same wavelength for solid and solution state. —: No discernible λ_{PL} was observed. [g] The second oxidation redox couples are irreversible for **6a**–**6g**. [h] The data were calculated from polymer film by the equation: gap = $1240/\lambda_{onset}$. [i] The HOMO energy levels were calculated from cyclic voltammetry and were referenced to ferrocene (4.8 eV). [j] LUMO = HOMO − gap.

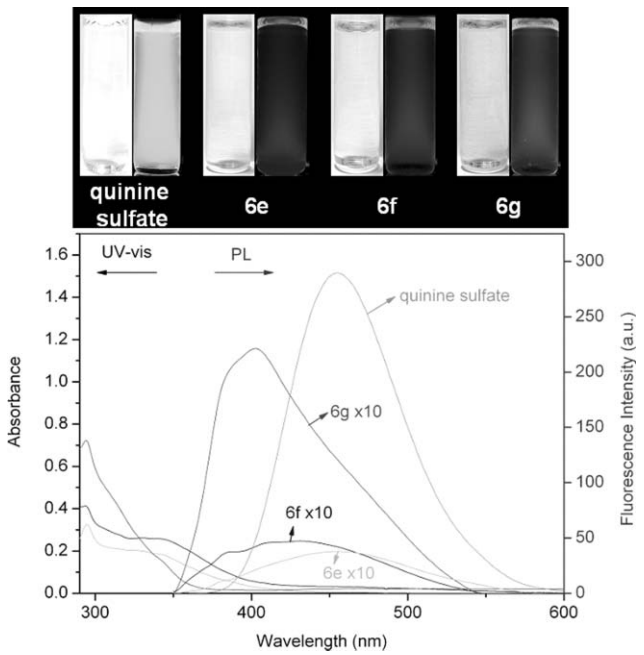

Fig. 7 UV-vis and PL spectra of solutions of poly(amine-imide)s **6e**, **6f**, and **6g** in NMP (1×10^{-5} M). A solution of quinine sulfate in 1 N H_2SO_4 (aq) with a concentration of 1×10^{-5} M was used as the reference standard (Φ_F = 0.546). Photographs show the appearance of the sample solutions before and after exposure to a standard laboratory UV lamp.

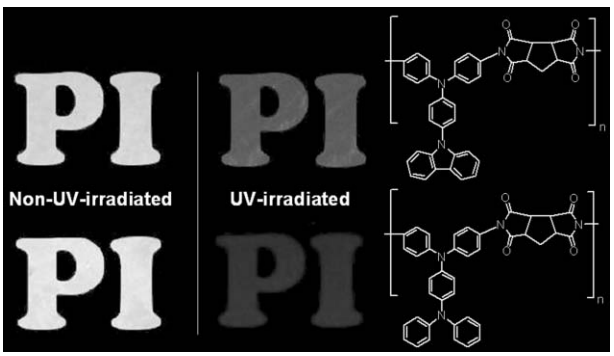

Fig. 8 Emission colors of the polymer films of **6g** and **6′g** when exposed to a standard laboratory UV lamp (λ around 365 nm, film thickness = 4–6 μm).

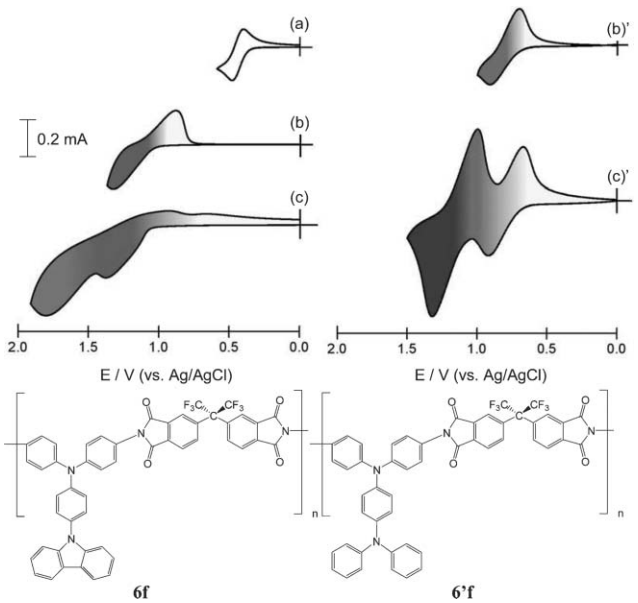

Fig. 9 Cyclic voltammograms of the cast films of poly(amine-imide) **6f** and **6′f** on an ITO-coated glass substrate in 0.1 M TBAP–CH_3CN at a scan rate of 100 mV s^{-1}. (a) Ferrocene; (b), (b)′ first redox couple; (c), (c)′ first and second redox couples.

Electrochromic characterization

Spectroelectrochemical analysis of the poly(amine-imide) films was carried out on an ITO-coated glass substrate, and they showed multicolor electrochromic behavior when the applied potential was changed. The color of the polymers was changed from neutral pale yellow or orange to green and to blue. The typical spectroelectrochemical behavior of poly(amine-imide) **6f** at various applied potentials is depicted in Fig. 10. When the applied potential was increased positively from 0.00 to 1.15 V, the peak of the characteristic absorbance at 312 nm for

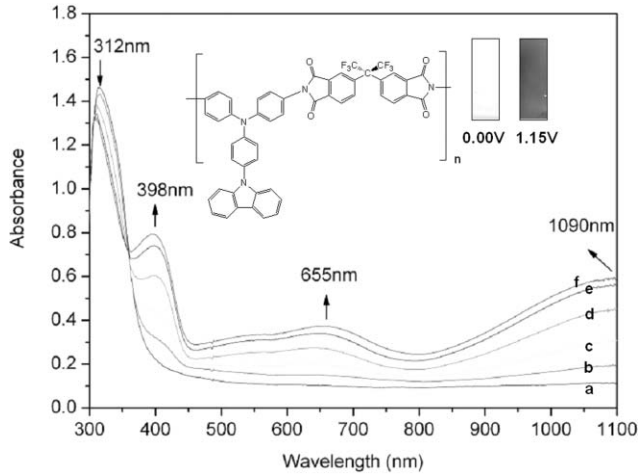

Fig. 10 *In situ* spectroelectrochemical series of a cast film of poly(amine-imide) **6f** in 0.1 M TBAP–CH_3CN at various applied potentials *vs.* Ag/Ag^+: (a) 0.00, (b) 0.90, (c) 1.00, (d) 1.05, (e) 1.10, and (f) 1.15 V.

poly(amine-imide) **6f** decreased gradually while three new bands grew up at 398, 655, and 1090 nm due to the first electron oxidation. The new spectrum was assigned as that of the stable cationic radical poly(amine-imide)$^{+\bullet}$. As the applied potential increased to the oxidation side, the film color changed from pale yellow to green (as shown in Fig. 10). The second oxidation generated electrochemically was not very stable as time passed at applied potentials higher than 1.35 V. When the applied potential was higher than 1.5 V, the film color was changed from green to dark blue.

The stability and response time upon electrochromic switching of the polymer film between its neutral and oxidized forms in the visible (398 and 655 nm) was monitored (Fig. 11). The color switching times were estimated by applying a potential step, and the absorbance profiles were followed. The switching time was defined as the time required to reach 90% of the full change in absorbance after switching potential. The thin film from poly(amine-imide) **6f** would require 3 s at 1.15 V for switching absorbance at 398 and 655 nm and 1.5 s for bleaching. After ten continuous cyclic scans between 0.00 and 1.15 V, the polymer films still exhibited excellent stability of electrochromic characteristics.

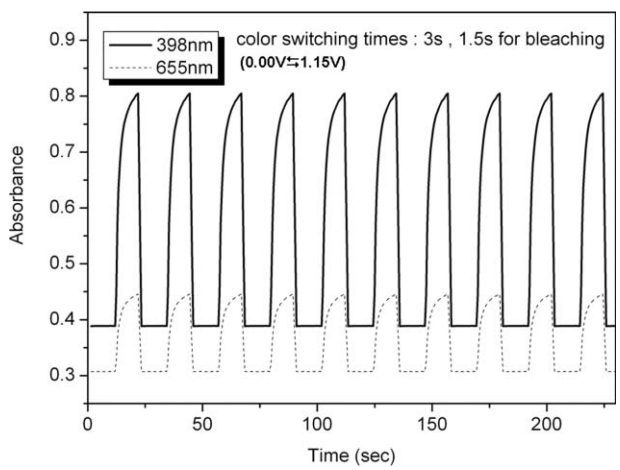

Fig. 11 Variation of absorbance for a cast film of poly(amine-imide) **6f** as a function of time for ten switches between 0.00 and 1.15 V *vs.* Ag/Ag^+ in 0.1 M TBAP–CH_3CN.

Conclusions

The new carbazole-based aromatic diamine monomer, 4,4′-diamino-4″-*N*-carbazolyltriphenylamine **4**, was successfully synthesized in high purity and good yield. Novel poly(amine-imide)s bearing pendent *N*-phenylcarbazole units were prepared by the two-step method starting from the diamine with various tetracarboxylic dianhydrides. All the poly(amine-imide)s were amorphous with high T_g and exhibited excellent thermal stability and useful mechanical properties (*e.g.* flexibility). The semi-aromatic poly(amine-imide) **6g** showed light color and high optical transparency and exhibited violet–blue photoluminescence both in film state and in NMP solution with about a 4.54% quantum yield. The poly(amine-imide) films showed good adherent behavior and were found to be electroactive. The multicolor electrochromic behavior of the polymer films exhibited pale yellow, green, and blue colors when various potentials were applied. All obtained poly(amine-imide)s revealed good stability of electrochromic characteristics for the first oxidation state, changing color from the yellowish neutral form to the green oxidized forms when scanning potentials positively from 0.00 to 1.15 V. Thus, our novel poly(amine-imide)s can be employed as potential candidates in the development of dynamic electrochromic and EL devices due to their suitable HOMO value, excellent thermal stability and reversible electrochemical behavior.

Acknowledgements

We are grateful to the National Science Council of the Republic of China for financial support of this work.

References

1 (*a*) C. W. Tang and S. A. VanSlyke, *Appl. Phys. Lett.*, 1987, **51**, 913; (*b*) C. W. Tang, S. A. VanSlyke and C. H. Chen, *J. Appl. Phys.*, 1989, **85**, 3610; (*c*) C. Adachi, K. Nagai and N. Tamoto, *Appl. Phys. Lett.*, 1995, **66**, 2679; (*d*) Y. Shirota, *J. Mater. Chem.*, 2000, **10**, 1; (*e*) Y. Shirota, *J. Mater. Chem.*, 2005, **15**, 79.

2 (*a*) E. Bellmann, S. E. Shaheen, S. Thayumannvan, S. Barlow, R. H. Grubbs, S. R. Marder, B. Kippelen and N. Peyghambarian, *Chem. Mater.*, 1998, **10**, 1668; (*b*) E. Bellmann, S. E. Shaheen, R. H. Grubbs, S. R. Marder, B. Kippelen and N. Peyghambarian, *Chem. Mater.*, 1999, **11**, 399; (*c*) J. P. Lu, A. R. Hlil, Y. Sun, A. S. Hay, T. Maindron, J.-P. Dodelet and M. D'Iorio, *Chem. Mater.*, 1999, **11**, 2501; (*d*) X. Q. Wang, M. Nakao, K. Ogino, H. Sato and H. M. Tan, *Macromol. Chem. Phys.*, 2001, **202**, 117; (*e*) X. Q. Wang, Z. J. Chen, K. Ogino, H. Sato, K. Strzelec, S. Miyata, Y. J. Luo and H. M. Tan, *Macromol. Chem. Phys.*, 2002, **203**, 739; (*f*) Q. Fang and T. Yamamoto, *Macromolecules*, 2004, **37**, 5894; (*g*) H. B. Xiao, B. Leng and H. Tian, *Polymer*, 2005, **46**, 5705; (*h*) J.-S. Cho, A. Kimoto, M. Higuchi and K. Yamamoto, *Macromol. Chem. Phys.*, 2005, **206**, 635; (*i*) M. H. Sun, J. Li, B. S. Li, Y. Q. Fu and Z. S. Bo, *Macromolecules*, 2005, **38**, 2651.

3 (*a*) Y. Q. Liu, M. S. Liu, X.-C. Li and A. K.-Y. Jen, *Chem. Mater.*, 1998, **10**, 3301; (*b*) X.-C. Li, Y. Q. Liu, M. S. Liu and A. K.-Y. Jen, *Chem. Mater.*, 1999, **11**, 1568; (*c*) M. Redecker, D. D. C. Bradley, M. Inbasekaran, W. W. Wu and E. P. Woo, *Adv. Mater.*, 1999, **11**, 241; (*d*) C. Ego, A. C. Grimsdale, F. Uckert, G. Yu, G. Srdanov

and K. Mullen, *Adv. Mater.*, 2002, **14**, 809; (*e*) C.-F. Shu, R. Dodda, F.-I. Wu, M. S. Liu and A. K.-Y. Jen, *Macromolecules*, 2003, **36**, 6698; (*f*) F.-I. Wu, P.-I. Shih, C.-F. Shu, Y.-L. Tung and Y. Chi, *Macromolecules*, 2005, **38**, 9028.
4 (*a*) Y.-J. Pu, M. Soma, J. Kido and H. Nishide, *Chem. Mater.*, 2001, **13**, 3817; (*b*) F. S. Liang, Y.-J. Pu, T. Kurata, J. Kido and H. Nishide, *Polymer*, 2005, **46**, 3767; (*c*) F. S. Liang, T. Kurata, H. Nishide and J. Kido, *J. Polym. Sci., Part A: Polym. Chem.*, 2005, **43**, 5765.
5 (*a*) T. Miteva, A. Meisel, W. Knoll, H. G. Nothofer, U. Scherf, D. C. Muller, K. Meerholz, A. Yasuda and D. Neher, *Adv. Mater.*, 2001, **13**, 565; (*b*) Y. Q. Fu, Y. Li, J. Li, S. K. Yan and Z. S. Bo, *Macromolecules*, 2004, **37**, 6395.
6 J. V. Grazulevicius, P. Strohriegl, J. Pielichowski and K. Pielichowski, *Prog. Polym. Sci.*, 2003, **28**, 1297.
7 H. Sasabe, *Supramol. Sci.*, 1996, **3**, 91.
8 J. F. Morin and M. Leclerc, *Macromolecules*, 2002, **35**, 8413.
9 Z.-B. Zhang, M. Fujiki, H.-Z. Tang, M. Motonaga and K. Torimitsu, *Macromolecules*, 2002, **35**, 1988.
10 S. Brizius, U. H. Kroth and F. Bunz, *Macromolecules*, 2002, **35**, 5317.
11 J. Bouchard, M. Belletele, G. Durocher and M. Leclerc, *Macromolecules*, 2003, **36**, 4624.
12 K. L. Paik, N. S. Baek and H. K. Kim, *Macromolecules*, 2003, **35**, 6782.
13 F. Sanda, T. Kawaguchi, T. Masuda and N. Kobayashi, *Macromolecules*, 2003, **36**, 2224.
14 K. Kim, Y.-R. Hong, S.-W. Lee, J.-I. Jin, Y. Park, B.-H. Sohn, W.-H. Kim and J.-K. Park, *J. Mater. Chem.*, 2001, **11**, 3023.
15 (*a*) Y. Zhang, T. Wada and H. Sasabe, *J. Polym. Sci., Part A: Polym. Chem.*, 1996, **34**, 2289; (*b*) Q. Wang, A. Gharvi, W. Li and L. Yu, *Polym. Prepr.*, 1997, **38**, 2, 516; (*c*) J. Jiang, C. Jiang, W. Yang, H. Zhen, F. Hung and Y. Cao, *Macromolecules*, 2005, **38**, 4072; (*d*) J. Huang, Y. Niu, W. Yang, Y. Mo, M. Yuan and Y. Cao, *Macromolecules*, 2002, **35**, 6080; (*e*) J.-F. Morin and M. Leclerc, *Macromolecules*, 2001, **34**, 4680.
16 (*a*) J. Gratt and R.-E. Cohen, *Macromolecules*, 1997, **30**, 3137; (*b*) J. Hwang, J. Sohn and S. Y. P, *Macromolecules*, 2003, **36**, 7970; (*c*) S. H. Hsiao, C. W. Chen and G. S. Liou, *J. Polym. Sci., Part A: Polym. Chem.*, 2004, **42**, 3302; (*d*) I. Mustonen, T. Hukka and T. Pakkanen, *Macromol. Rapid Commun.*, 2000, **21**, 1286; (*e*) Z. Chen, Y. Liu, C. Zhang and F. Bai, *J. Appl. Polym. Sci.*, 2004, **92**, 2777.
17 (*a*) *Polyimides*, ed. D. Wilson, H. D. Stenzenberger and P. M. Hergenrother, Blackie, Glasgow and London, 1990; (*b*) *Polyimides: Fundamentals and Applications*, ed. M. K. Ghosh and K. L. Mittal, Marcel Dekker, New York, 1996.
18 (*a*) F. W. Harris and S. L.-C. Hsu, *High Perform. Polym.*, 1989, **1**, 1; (*b*) Y. Imai, *React. Funct. Polym.*, 1996, **30**, 3; (*c*) S. H. Hsiao and C. T. Li, *Macromolecules*, 1998, **31**, 7213; (*d*) G. S. Liou, *J. Polym. Sci., Part A: Polym. Chem.*, 1998, **36**, 1937; (*e*) G. C. Eastmond, J. Paprotny and R. S. Irwin, *Polymer*, 1999, **40**, 469; (*f*) G. C. Eastmond, M. Gibas and J. Paprotny, *Eur. Polym. J.*, 1999, **35**, 2097; (*g*) D. S. Reddy, C. H. Chou, C. F. Shu and G. H. Lee, *Polymer*, 2003, **44**, 557; (*h*) B. Y. Myung, C. J. Ahn and T. H. Yoon, *Polymer*, 2004, **45**, 3185.
19 G. S. Liou, S. H. Hsiao, M. Ishida, M. Kakimoto and Y. Imai, *J. Polym. Sci., Part A: Polym. Chem.*, 2002, **40**, 3815.
20 S. H. Cheng, S. H. Hsiao, T. H. Su and G. S. Liou, *Macromolecules*, 2005, **38**, 307.
21 E. T. Seo, R. F. Nelson, J. M. Fritsch, L. S. Marcoux, D. W. Leedy and R. N. Adams, *J. Am. Chem. Soc.*, 1966, **88**, 3498.
22 L. Hagopian, G. Kohler and R. I. Walter, *J. Phys. Chem.*, 1967, **71**, 2290.
23 A. Ito, H. Ino, K. Tanaka, K. Kanemoto and T. Kato, *J. Org. Chem.*, 2002, **67**, 491.
24 H. Tachimori and T. Masuda, *J. Polym. Sci., Part A: Polym. Chem.*, 1995, **33**, 2079.
25 J. P Chen and A. Natansohn, *Macromolecules*, 1999, **32**, 3171.
26 J. N. Demas and G. A. Crosby, *J. Phys. Chem.*, 1971, **75**, 991.
27 T. Matsumoto and T. Kurosaki, *Macromolecules*, 1997, **30**, 993.

